Synthetic Metals 159 (2009) 813–816

Contents lists available at ScienceDirect

Synthetic Metals

journal homepage: www.elsevier.com/locate/synmet

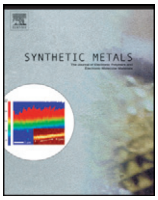

Quantum size titanium oxide templated with a π-conjugated dendrimer: crystal structure in the quantum size domain

Norifusa Satoh, Kimihisa Yamamoto*

Department of Chemistry, Faculty of Science of Technology, Keio University, 3-14-1 Hiyoshi, Yokohama 223-8522, Japan

ARTICLE INFO

Article history:
Received 20 November 2008
Received in revised form 24 December 2008
Accepted 9 January 2009
Available online 7 February 2009

Keywords:
Dendrimer template
Metal oxide nanoparticles
Quantum size effect

ABSTRACT

Metal-based nanoparticles templated with dendrimers have recently attracted much interest to control particle sizes strictly. However, the standard deviation of the obtained particles is larger than that of the single-mass Au clusters (0.2 nm). We succeeded the subnanosize-control of TiO_2 particles (both of rutile and anatase crystal structures based on the difference in the synthesis methods) with a standard deviation of 0.2 nm, using finely controlled metal assembly on a phenylazomethine dendrimer (DPA G4). The optical absorption spectra of the obtained particles revealed that the quantum size effect and the difference in the crystal structure, such as rutile and anatase, exists less than 2 nm particle sizes. A semi-empirical effective mass approximation, introduced a new concept; apparent reduced mass, describes the size dependency and the difference based on the crystal structure in the bandgap energy of the indirect and direct transition.

1. Introduction

There have never been nanotechnology to control particle sizes based on the number of the components. The usual methods to prepare particles are based on thermodynamic collision under gas or solution phases, resulting in the statistical distribution. Thus, dendrimer templates have attracted much attention to prepare metal-based nanoparticles within the restricted inner space because of the perfectly regulated structure [1]. However, the number and location of the metal ions tend to be random within each dendrimer. Thus, the standard deviation of the obtained particles is larger than that of the single-mass Au clusters (0.2 nm) [2,3]. Recently, we developed a fourth generation phenylazomethine dendrimer (DPA G4: Fig. 1), in which the complexation of 30 metal ions (as metal chlorides) proceeds in a radial stepwise manner [4]. The stepwise progression means that the complexation never occurs in the outer layers until the inner layers are initially occupied. Thus, the number and location of metal ions can be finely controlled in the DPAs. By using the DPA G4 as a template, we should be able to achieve a greater size-control with a narrower size distribution [5].

Titanium oxide (TiO_2) is classified as an indirect bandgap semiconductor; a weak absorption by the indirect transition is observed from a lower energy point (3.0 eV for rutile and 3.2 eV for anatase) than a strong absorption by the direct transition bandgap (3.3 eV for rutile [6] and 3.4 eV for anatase [7,8]) in bulk. Nanoparticles of indirect semiconductors would be considered to change the transition nature into direct one with decreasing in size, because the structure finally reaches the molecular size having a direct transition property. Serpone et al. inferred that the blue shift of TiO_2 nanoparticles should be based not on the quantum size (Q-size) effect but on the change into the direct transition because of the observation of the size-independent blue shift using the size-uncontrolled samples ($2R = 2.1 \pm 1.1$ nm, 13.3 ± 4.5 nm, and 26.7 ± 9.0 nm) [9]. However, this insistence is unacceptable because of the experimental error due to the enormous large size-distribution. The samples containing 5 nm particles show almost bulk bandgap energy (Fig. 2A). Additionally, they assigned the absorption spectra of the anatase particles using the band calculation for the rutile single crystal [10] (Fig. 2B).

2. Theoretical model

The following relationship between the bandgap of a semiconductor particle (E_{infinite}) and the radius (R) is described by Brus, using the effective mass approximation [11]:

$$E_{\text{infinite}} \equiv E_g + \frac{\hbar^2\pi^2}{2R^2}\frac{1}{\mu} - \frac{1.8e^2}{\varepsilon R} + \text{smaller terms} \qquad (1)$$

where $\hbar$ is Planck's constant; e is the charge on the electron; E_g is the bandgap in the bulk; μ is the reduced mass of the electron m_e and hole m_h in the bulk; and ε is the dielectric constant of the bulk semiconductor. The failure of the Brus equation is generally known especially in the ultrasmall region (quantum size domain: size region under the exciton radius [12]); for example, in the case of

---

* Corresponding author. Tel.: +81 45 566 1718; fax: +81 45 566 1718.
E-mail address: yamamoto@chem.keio.ac.jp (K. Yamamoto).

0379-6779/$ – see front matter © 2009 Elsevier B.V. All rights reserved.
doi:10.1016/j.synthmet.2009.01.012

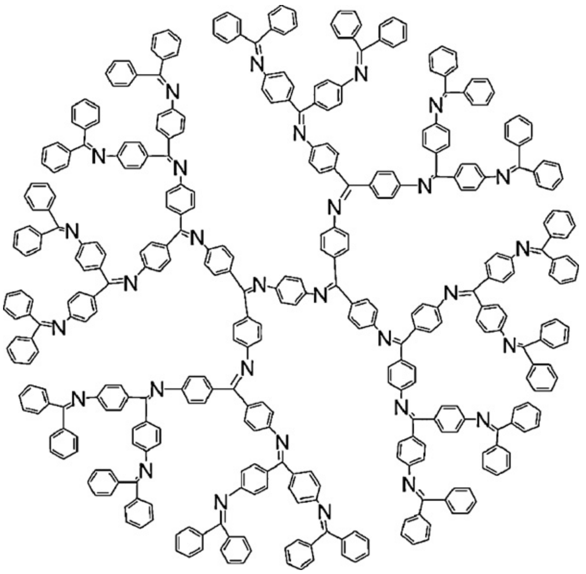

Fig. 1. Molecular structure of DPA G4.

CdS. The main reason is the conventional infinite depth well model of the Brus equation.

Assuming an apparent reduced mass of the electron and hole μ' and an apparent dielectric constant ε' in the infinite depth well model, we can replace the Nosaka equation [13] for the excitation energy E_{finite} using a finite depth well model with the following expression looking like a Brus equation:

$$E_{\mathrm{finite}} \sim E_{\mathrm{g}} + \frac{\hbar^2\pi^2}{2R^2}\frac{1}{\mu'} - \frac{1.8e^2}{\varepsilon' R} \qquad (2)$$

In the case of TiO_2, the normally used value of $1.63m_{\mathrm{o}}$ as the μ in the Brus equation would be the above μ' to describe the realistic finite potential well model in the rigorous meaning. Because the value is experimentally estimated by Kormann et al. [12], using quantum size titanium oxide (Q-size TiO_2), which shows the blue shift, $\Delta E = 0.15$ eV at $R = 1.2$ nm. As Kormann et al. also mentioned, the real μ is believed to be less than 1 m_{o} in the bulk because m_{h} is much smaller than m_{e} (e.g., m_{e} ~5–100 m_{o}, m_{h} ~0.01–0.8 m_{o}) [14,15]. Especially, the ε in TiO_2 is large enough to permit ignoring the failure due to the infinite depth well model because of the small second term of the Brus equation (cf. $\varepsilon = 5.7$ for CdS). For these reasons, the Brus equation for TiO_2, generally adopted, would correspond to the experimental data. Namely, the Eq. (2) is not the Brus equation based on the infinite depth well model but is equivalent to the Nosaka equation based on the finite depth well model in physical meaning.

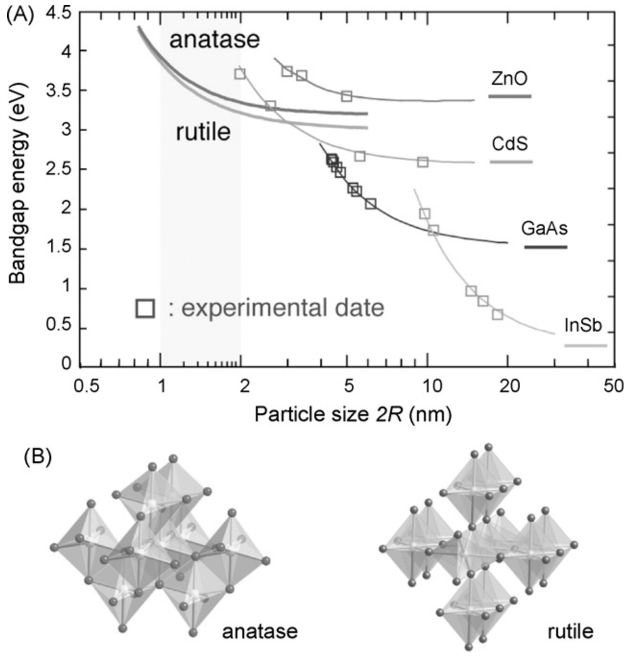

Fig. 2. (A) Calculated size-dependency and experimental date for TiO_2 and other semiconductors in bandgap energy. (B) Difference in the crystal structure between anatase (zigzag chain) and rutile (linear chain).

Additionally, this kind of semi-empirical prediction would essentially include the information about the surface and the atomic character of the nanoparticles under the same condition. Zunger and co-author succeed in treating these problems in the calculation of the electronic structure, using the semi-empirical pseudopotential method [16]. Experimentally, it has been shown that the surface modification of nanoparticles, e.g., CdSe and CdS, has little effect on the absorption spectra without the electronic interaction with the aromatic rings of the surface-capping molecules [17,18]. As showing in Fig. 2A, the semi-empirical effective mass approximation can describe the size-dependent bandgap energy observed experimentally in other semiconductors [19–22].

3. Experiment

DPA G4 and phenylazomethine were prepared according to a previous method [23]. $Ti(acac)Cl_3$ was synthesized following a literature method [24]. All other chemicals were purchased from Kantoh Kagaku Co. and used as received. UV–vis spectra were recorded using a Shimadzu UV-3100PC spectrometer with a closed quartz cell (optical path length: 1 cm). AFM was performed using a SII SPA400 instrument under ambient conditions with the tapping mode of imaging (DFM). Si probes having a spring constant of 42 N/m (SII SI-DF40P for DFM) were used at a resonance frequency of 300 kHz. A 20-μm scanner (SPA400-PZT (FS-20A), 970P3202) was used. The TEM images were obtained at 120 kV with a JEOL JEM-2010 instrument. The OWG spectra were obtained using a System Instruments Co., Ltd., SIS-5000 spectrophotometer.

Synthesis of Q-size TiO_2. The chloroform–acetonitrile (v/v = 1/1) solution of the Ti-assembled DPA G4 (5×10^{-6} M) was filtered through a membrane filter (0.2 μm), and then cast on TEM grids (1 μl) for the TEM, on a quartz plate as the optical waveguide for the OWG spectroscopy (<4 μl/cm^2), and spun on mica substrates for the AFM (4 μl, 2000 rpm). To prevent molecular aggregation on the substrates, we determined the maximum coverage, 4 μl/cm^2, considering the size of the Ti-assembled DPA G4 calculated from the molecular modeling. For hydrolysis, the substrates were exposed to the vapors of a 10% HCl solution in a chamber at room temperature for 1 h, annealed at 500 °C for 1 h (with the exception of the TEM grids because of heat weakness), and then treated within a UV/O_3 chamber (Technovision, Inc., Model 208 UV-O_3 cleaning system) for 10 min. For thermolysis, the substrates were annealed at 500 °C for 1 h, and then treated within the UV/O_3 chamber for 10 min.

4. Results and discussion

The radial stepwise complexation of $Ti(acac)Cl_3$ into the DPA G4 dendrimer was observed until a stoichiometric amount (per imine site) of $Ti(acac)Cl_3$ had been added. Four distinct transitions could be identified at the isosbestic points: 363 nm, 0–2 equiv.; 361 nm, 3–6 equiv.; 358 nm, 7–14 equiv.; 353 nm, 15–30 equiv. The number of added equivalents of $Ti(acac)Cl_3$ at each transition is consistent with that of the imine sites present in the different layers of DPA G4.